An evaluation of the role of miR-361-5p in senescence and systemic ageing

Emad Manni [a], Nicola Jeffery [a], David Chambers [b], Luke Slade [c], Timothy Etheridge [c], Lorna W. Harries [a,*]

[a] University of Exeter Medical School, Faculty of Health and Life Sciences, Barrack Road, Exeter EX2 5DW, UK
[b] Wolfson Centre for Age-Related Diseases, King's College London, London WC2R 2LS, UK
[c] Department of Sport and Health Sciences, College of Life and Environmental Sciences, University of Exeter, Exeter EX1 2LU, UK

ARTICLE INFO

ABSTRACT

Senescent cells are key regulators of ageing and age-associated disease. MicroRNAs (miRs) are a key component of the molecular machinery governing cellular senescence, with several known to regulate important genes associated with this process.

We sought to identify miRs associated with both senescence and reversal by pinpointing those showing opposing directionality of effect in senescence and in response to senotherapy. Cellular senescence phenotypes were assessed in primary human endothelial cells following targeted manipulation of emergent miRNAs. Finally, the effect of conserved target gene knockdown on lifespan and healthspan was assessed in a C. elegans system in vivo.

Three miRNAs (miR-5787, miR-3665 and miR-361-5p) demonstrated associations with both senescence and rejuvenation, but miR-361-5p alone demonstrated opposing effects in senescence and rescue. Treatment of late passage human endothelial cells with a miR-361-5p mimic caused a 14 % decrease in the senescent load of the culture. RNAi gene knockdown of conserved miR-361-5p target genes in a C. elegans model however resulted in adverse effects on healthspan and/or lifespan.

Although miR-361-5p may attenuate aspects of the senescence phenotype in human primary endothelial cells, many of its validated target genes also play essential roles in the regulation or formation of the cytoskeletal network, or its interaction with the extracellular matrix. These processes are essential for cell survival and cell function. Targeting miR-361-5p alone may not represent a promising target for future senotherapy; more sophisticated approaches to attenuate its interaction with specific targets without roles in essential cell processes would be required.

1. Introduction

Organismal ageing and its associated biochemical and cellular changes are major risk factors for the development of common, complex disease (Fougere et al., 2017). It is now becoming apparent that age-related disorders share a common set of triggers (Kenessary et al., 2013). The factors leading to ageing remain elusive, but there are consistent changes in cell biology that occur in ageing cells, which are known collectively as the 'hallmarks of ageing'. The original hallmarks include alteration of intracellular communication, stem cell exhaustion, genomic instability, shortening of telomere length, loss of proteostasis, epigenetic alteration, dysregulation of nutrient sensing, malfunction of mitochondria, and cellular senescence (Lopez-Otin et al., 2013). More recently, additional hallmarks including compromised autophagy,

microbiome disturbance, altered mechanical properties, inflammation and splicing dysregulation have been proposed (Schmauck-Medina et al., 2022).

Cellular senescence is defined as the irreversible exit from cell cycle that occurs at the end of the replicative lifespan of a cell. Senescent cells are alive and metabolically active, but exhibit characteristic differences to their non-senescent counterparts (Childs et al., 2017). These include morphological and functional changes, which in most cases include the secretion of the senescence-associated secretory phenotype (SASP); a cocktail of cytokines and remodeling proteins (Watanabe et al., 2017). The most compelling evidence for senescent cells as drivers of ageing involve selective ablation of senescent cells in transgenic mice demonstrated elegantly that the presence of such cells shortened healthy lifespan (Baker et al., 2016) and the removal of these is able to prevent

several age-associated diseases (Baker et al., 2011). Follow on work has since demonstrated links between the presence of senescent cells and multiple ageing phenotypes (Bussian et al., 2018; van Willigenburg et al., 2018; Ogrodnik et al., 2017). Accordingly, approaches to selectively ablate or regenerate senescent cells in vivo (senotherapeutics) are now the subject of intense study as future therapeutics which are already demonstrating promise in human systems (Justice et al., 2019; Paez-Ribes et al., 2019).

Cellular senescence can arise from repeated and unresolved cellular stress (He and Sharpless, 2017). Cells have a battery of molecular responses to stress, one of which is the microRNA (miRNA) response (LaPierre and Stoffel, 2017; Du et al., 2019). MicroRNAs are small RNA molecules of approximately 22 nucleotides in length that are pivotal regulators of gene expression and have roles in many aspects of cell development, proliferation, and apoptosis (Bartel, 2004). In accordance with their fundamental importance in complex cellular processes and in systemic ageing, studies have reported associations between miRNA profiles and age-related phenotypes (Grillari et al., 2010; Li et al., 2016; Rani et al., 2017), and between individual miRNA and cellular senescence itself (Pitto et al., 2009; Chen et al., 2020). The small size of miRNA, the relative ease of high throughput methods for measuring them and the ready availability of reagents for their evaluation in vitro has highlighted them as a promising therapeutic avenue (Chakraborty et al., 2017).

In this study, we aimed to identify miRNAs contributory to the establishment of senescence, and to characterize the effect of targeted manipulation of candidate miRNAs in vitro and of their validated target genes in vivo. We first sought to identify miRNAs demonstrating opposing directionality of expression in senescent primary human endothelial cells, and in those that had undergone small-molecule induced partial rejuvenation. We then evaluated the effect of targeted manipulation of miRNAs displaying opposing direction of effect in senescence and rejuvenation on senescence phenotypes in primary human endothelial cells in vitro. Finally, we determined the effect of knockdown of target genes of candidate miRs on lifespan and healthspan measures in an invertebrate model system *C. elegans*. We identified 3 miRNAs (miR-5787, miR-3665 and miR-361-5p) which demonstrated dysregulated expression in both datasets, but only one, miR-361-5p, exhibited opposing directionality. Treatment of primary senescent endothelial cell cultures with an miR-361-5p mimic to replicate expression levels in early passage cells brought about a reduction in senescent cell load of the culture. We determined that 65 validated miR-361-5p target genes were expressed in human primary endothelial cells, of which 32 demonstrated differential expression in senescent cells. 16 senescence-related miR-361-5p target genes had direct *C. elegans* orthologues, many of which were involved in regulation of cytoskeletal function and interaction with the extracellular matrix. Targeted RNAi gene knockdown of these revealed that 9/16 had statistically significant adverse effects on lifespan. Furthermore, 14/16 miR-361-5p target genes also reduced healthspan, as measured by decreased movement. Our work suggests that although miR-361-5p may be contributory to the senescent cell phenotype, its downstream targets include multiple genes that are essential for cellular health and function, meaning that simply elevating its expression is unlikely to be fruitful as a senotherapeutic approach.

2. Materials and methods

2.1. Cell culture conditions and assessment of senescence kinetics

Commercially procured primary human aortic endothelial cells (HAoEC; C-12271, PromoCell, Germany) were cultured and propagated in C-22022 medium (PromoCell, Germany) with 1 % penicillin and 1 % streptomycin at 37 °C and 5 % CO_2. Replicative senescence was induced by continuous culture as previously described until growth slowed to <0.5 population doublings per week (Holly et al., 2013; Latorre, 2017).

Early and late passage cells were at PD = 36 and PD = 84 respectively. For assessment of miRNA response to partial rejuvenation, we assessed response to 5 μM of resveratrol, a polyphenol previously demonstrated to lead to reversal of multiple senescence phenotypes in human primary dermal fibroblasts (Latorre, 2017) or with DMSO carrier alone for 48 h. Cells were seeded at a density of 4.0×10^5 cell/cm^2 in 6-well plates and left to settle for 24 h prior to treatment.

Senescence was evaluated at 80 % confluence by the Senescence Cells Histochemical Staining Kit (Sigma, Aldrich, UK; CS0030) (SA-β-Gal) in 3 biological replicates. Proliferation index and DNA damage foci were also assessed by Ki67 and γH2AX immunofluorescence in 3 biological replicates. In brief, cells were grown on 13 mm coverslips prior to fixation with 4 % paraformaldehyde. Primary antibodies were applied at 2.5 μg/mL for 24 h. After washing, secondary antibodies were applied at 5 μg/mL and DAPI at 1 μg/mL for 1 h. Coverslips were mounted using Dako mounting medium (S302380–2, Agilent). Antibodies were sourced from Abcam: Rb anti-Ki67 (ab15580, ab16667), Ms. anti-γH2AX (ab26350), Alexa Fluor ® 555 pAb to Rb (ab150078, ab150086) and Alexa Fluor ® 488 pAb to Ms. (ab150117). Images were captured using the Leica DM4 B Upright Microscope. Statistical significance was determined by one-way AVOVA in GraphPad Prism 8 (GraphPad Software, San Diego, California USA). A minimum of 5 representative image fields were manually counted for each assay, with a minimum of 400 cells assessed for each replicate.

2.2. RNA extraction and purification

Prior to RNA extraction, cells were washed in Dulbecco's phosphate-buffered saline (DPBS) and harvested. Total RNA was then extracted from each biological replicate using 1 mL of Tri reagent® (Thermo Fisher, Waltham, MA, USA) according to the manufacturer's instructions. RNA samples destined for GeneChip miRNome and whole transcriptome analysis were purified further using a RNA Clean & Concentrator kit (Zymo Research, CA, USA) according to the manufacturer's instructions.

2.3. Whole miRNome profiling

Transcriptome-wide miRNA patterns of miRNA expression were assessed in early passage (PD = 36), late passage (PD = 84) cells, and in resveratrol or vehicle (DMSO) treated late passage cells (PD = 84) in 3 biological replicates using the GeneChip™ miRNA 4.0 system (Thermo Fisher, Waltham, MA, USA), which allows simultaneous assessment of all miRNAs in miRBase release 20. Sample preparation and gene chip cartridge arrays were performed by a commercial subcontractor (UK Bioinformatics Ltd., Caterham, UK). Data underwent quality control for probeset mean for hybridization intensity, probeset residual mean which compares probeset signal to residual signal, poly-A positive spike in controls as control genes and positive versus negative area under the curve. SST-RMA was selected to reduce background and normalize intensity (46) following which a differential expression analysis was undertaken using the Transcriptomic Analysis Console (TAC) (Applied Biosystems) software (TAC 4.0.2.10) using the default settings (22, 47). Differences between two groups were identified by one-way ANOVA. Data analysis and statistical significance were completed using Graph-Pad Prism 8.0 software (GraphPad Software, La Jolla, CA, USA). Data were adjusted for false discovery rate by Benjamini Hochberg correction.

2.4. qRTPCR validation of miR-361-5p expression in senescent cells

To validate our microarray results, we carried out quantitative PCR assessment of the expression of miR-361-5p in a previously untested set of early passage (PD = 36) and late passage (PD = 84) human primary endothelial cells. Assay details are available on request. Cells were assessed in three biological and three technical replicates. Quantitative

RTPCR reaction mixes included 2.5 µL Taqman® Universal PCR mastermix II (no AmpErase® UNG) (Thermo Fisher, Waltham, MA, USA), 1.75 µL dH$_2$O, 0.5 µL cDNA and 0.25 µL Taqman® gene assay (Thermo Fisher, Foster City USA) in a 5 µL reaction volume. Cycling conditions were: 50 °C for 2 min, 95 °C for 10 min and 50 cycles of 15 s at 95 °C for 30 s and 1 min at 60 °C. Reactions were carried out in 3 biological replicates and 3 technical replicates. Endogenous controls were chosen on the basis that they did not display expression change in senescent cells and were miR-24, miR-15 and miR-10b. The relative expression of each target miRNA was determined by the comparative Ct approach and was calculated relative to the geometric mean of the endogenous control genes.

2.5. Identification of miR-361-5p target genes and assessment of their expression in senescence

To assess the genuine gene targets of miR-361-5p, we used the DNA intelligent analysis (DIANA) mirPath v3.0 database (Paraskevopoulou et al., 2013; Vlachos et al., 2015), which identifies target genes across multiple prediction programs, and the miRTarBase version 9.0 platform, a database containing only experimentally validated miRNA target genes (Huang et al., 2020; Huang et al., 2022). All identified target genes were then assessed for expression in human primary endothelial cells and for expression changes in relation to cellular senescence in 3 biological replicates of early and late passage human primary endothelial cells (PDs 36 and 84 respectively). Expression levels of validated miR-361-5p target genes were assessed on the Clariom D Pico GeneChip platform (Thermo Fisher, Waltham, MA, USA) as described above. Sample preparation and gene chip cartridge arrays were performed by a commercial subcontractor (UK Bioinformatics Ltd., Caterham, Surrey). Data QC was carried out as described above to ensure data normality and clustering, and associations between the expression of validated target genes and cellular senescence was then analyzed using TAC 4.0.2.10 (Applied Biosystems, Thermo Fisher, Waltham, MA, USA).

2.6. Manipulation of miR-361-5p levels using a miRNA mimic

To determine whether restoring miR-361-5p levels in senescent primary endothelial cells was capable of attenuating senescence, aged cells at PD80 were seeded into 12 well plates at a density of 2×10^5 cells/well and maintained until 70 % confluence. Cells were then transfected with 50 pmol of a MirVana mimic (Thermo Fisher, Waltham, MA, USA) to miR-361-5p for 24 h. Transfections were carried out using Lipofectamine 3000 (Thermo Fisher, Waltham, MA, USA) and lipofectamine-only and scramble controls were also performed. The percentage of senescent cells in the culture was then assessed by senescence-associated beta galactosidase staining in duplicate fields of each of 3 biological replicates, with >400 cells per condition assessed. Differences between treated and control cultures assessed for statistical significance by unpaired *t*-test (SPSS v26, IBM statistics).

2.7. Gene ontology pathway analysis of dysregulated miRNA target genes

Gene Set enrichment analysis (GSEA) was carried out to identify pathways that were enriched in senescence-associated miR-361-5p target genes, but also separately for targets of the senescence or resveratrol regulated miRNome. Target genes of validated miRNAs were identified using miRTarBase (Huang et al., 2020; Huang et al., 2022) and then confirmed to demonstrate altered expression in senescence or reversal as appropriate. Validated targets were then queried for enrichment in specific cellular, molecular or biological function Gene Ontology (GO) pathways using EnrichR, a webtool designed to determine whether candidate genes from a user-supplied list are present in specific pathways or processes than one would expect by chance (Chen et al., 2013). Demonstration of enrichment was based on the adjusted *p* value significance, with ranking derived from Fisher exact test).

2.8. Assessment of the effect of targeted knockdown of miR-361-5p target genes on lifespan and healthspan in C. elegans

C. elegans orthologues corresponding to validated miR-361-5p target genes were identified by comparison of two different databases to maximize the chances of identifying the correct orthologue. Databases were the NCBI HomoloGene database (ncbi.nlm.nih.gov/homologene; Release 68) and the Ortholist 2 database (ortholist.shaye-lab.org), which is based on a meta-analysis of six different orthology-prediction algorithms (Kim et al., 2018). 16 miR-361-5p target genes had validated *C. elegans* orthologues. These were: *rho-1 (RHOA)*, *deb-1 (VCL)*, *daf1 (TGFBR1)*, *ifa-1 (VIM)*, *cyk-1 (DIAPH1)*, *hlh-8 (TWIST1)*, *erm-1 (EZR)*, *atn-1 (ACTN4)*, *let-805 (FN1)*, *sdn-1 (SDC4)*, *wsp-1 (WASL)*, *C46H11.3 (ARPC5L)*, *dgn-2 (DAG1)*, *pes-7 (IQGAP1)*, *hrdl-1 (AMFR)* and *sup-46 (HNRNPM)*. Wild-type Bristol nematodes (N2 Bristol) were obtained from the *Caenorhabditis* Genetics Centre and were maintained on nematode growth media (NGM) plates plated with *Escherichia coli* OP50 at 20 °C according to previously described methods (Brenner, 1974). Animals were age-synchronized by gravity synchronization from the L1 stage. RNAi clones were procured from the Ahringer repository (Kamath and Ahringer, 2003) and delivered to the animals in 20 mg/mL of *E. coli* OP50 bacteria in liquid NGM. Synchronized L1 larvae were plated on RNAi NGM plates containing (50 mM NaCl, 0.25 % (*w/v*) bacto peptone, 1.7 % (w/v) agar, 1 mM CaCl2, 1 mM MgSO4, 25 mM KH2PO4 (pH 6), 12.9 µM cholesterol, 1 mM IPTG, 50 µg/mL ampicillin. Empty vector was included as a negative control, and *daf-16* was included as a positive control.

2.9. Microfluidic assessment of C. elegans lifespan and healthspan

The effects of knockdown of the *C. elegans* orthologues of validated miR-361-5p target genes on lifespan and healthspan parameters was measured using the microfluidics-based Infinity Screening System (NemaLife Inc.) (Rahman et al., 2020; Rahman, 2019) on RNAi-treated worms. Worms were grown to day 0 of adulthood on RNAi NGM plates according to established protocols (Ellwood et al., 2021) and then washed 3 times with M9 buffer to allow separation of young adult animals from bacterial contaminants and collected in 2.5 mL syringes. 60–70 worms were loaded onto each chip according to manufacturer's instructions (Rahman et al., 2020). Survival and movement analysis was carried out daily; chips were washed to remove progeny prior to assessment of survival and movement for 90s. Survival and movement analysis was assessed from 3 still-image frames per chip taken at 30 s intervals using a 0 to 1 coefficient in the Infinity Systems software (NemaLife Inc., Texas) with dead animals indicated by a coefficient of 0 and inactive animals indicated with coefficients of 0.01 to 0.40. Animals scoring between coefficients of 0.40 and 1 were classified as active, mobile animals. Data were normalized to the number of animals loaded on day 1 of adulthood.

3. Results

3.1. Senescence kinetics of early passage, late passage and rejuvenated primary human endothelial cells

Early passage human primary endothelial cells (PD = 36) demonstrated an average level of 10 % SA-β-Gal positive cells, whereas late passage cells (PD = 84) demonstrated 64 % positivity ($p = 0.0001$). This was accompanied by a 25 % decrease in the number of cells staining positive for the cell proliferation marker Ki67 ($p = 0.0008$) and a 28 % increase in the number of cells demonstrating γH2AX foci indicating increased levels of DNA damage ($p = 0.0155\ 01$; Fig. 1). We have previously reported that resveratrol and related analogues are able to bring about attenuation of multiple senescence phenotypes in late passage human primary dermal fibroblasts (Latorre, 2017). We observed a similar effect in human primary endothelial cells with treated cells
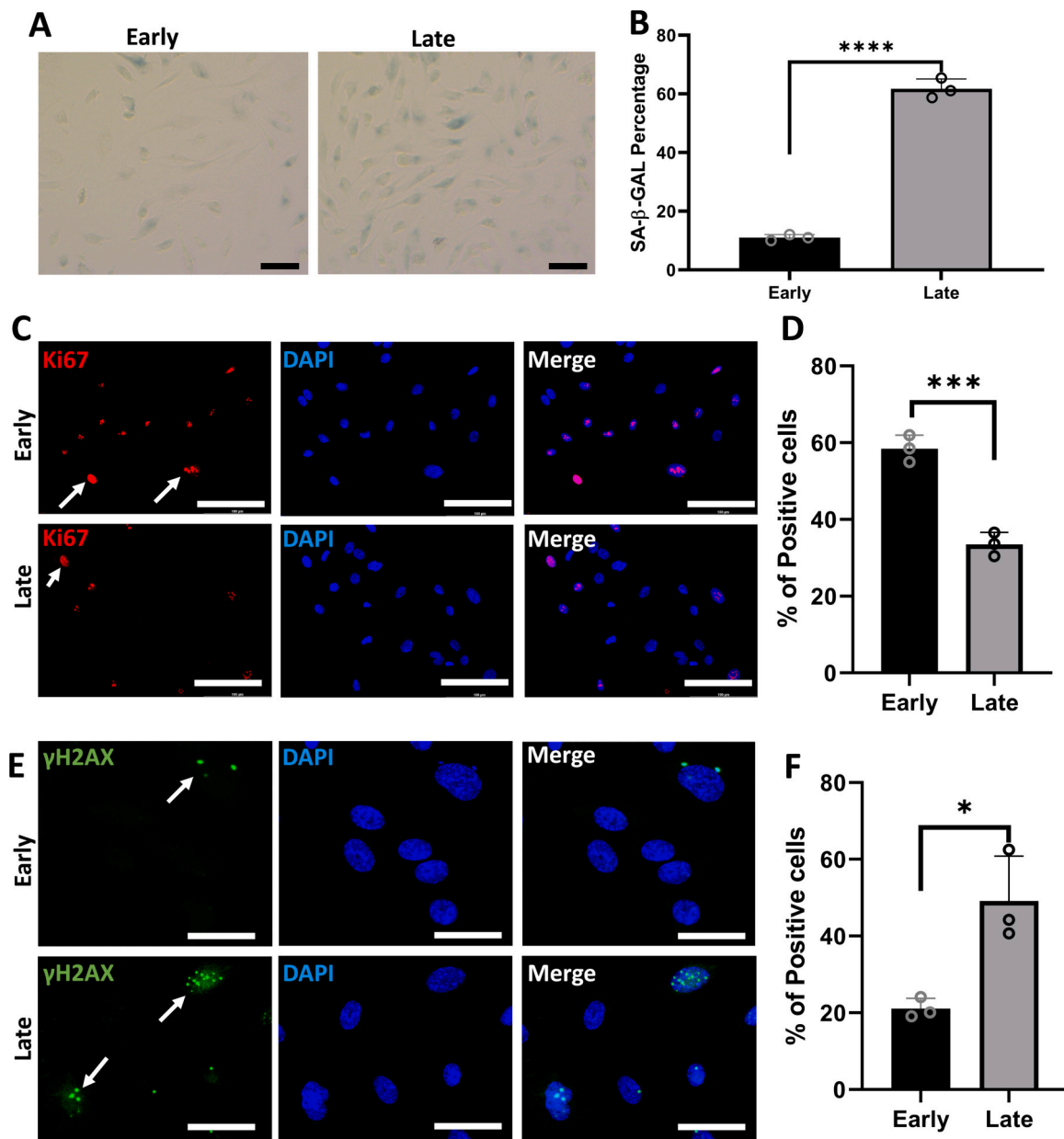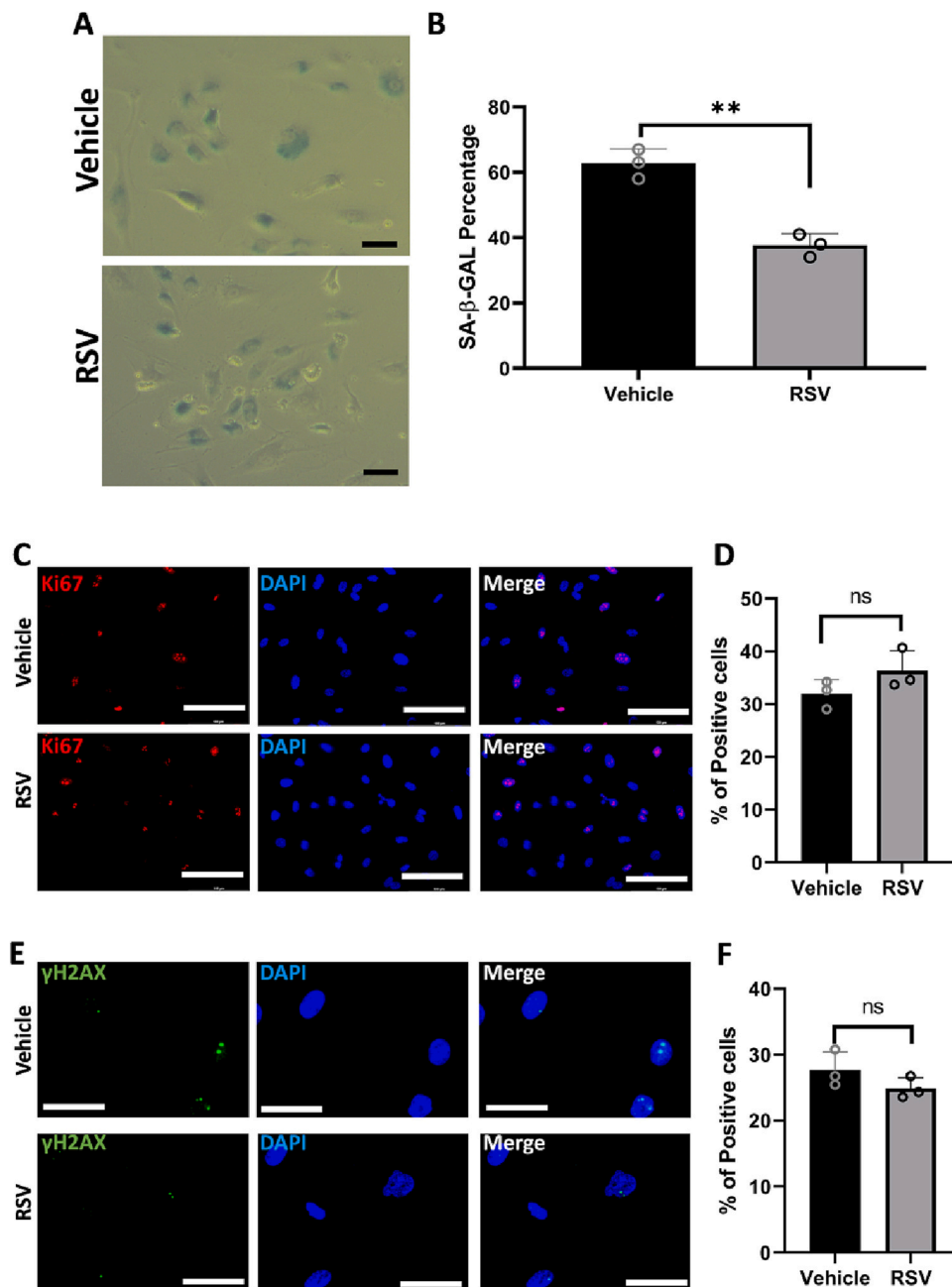
Fig. 1. Senescence kinetics of early and late passage human primary endothelial cells. (A) Microscope fields illustrating representative senescence-associated beta galactosidase (SA-β-Gal) activity in early (PD = 36) and late passage (PD = 84) human primary endothelial cells. (B) Graph showing change in SA-β-Gal activity in early and late passage human primary endothelial cells. (C) Proliferation kinetics in early (PD = 36) and late passage (PD = 84) human primary endothelial cells stained for Ki67 activity. (D) Graph showing change in Ki67 staining in in early and late passage human primary endothelial cells. (E) DNA damage foci as identified by γH2AX staining in early and late passage human primary endothelial cells. (F) Graph showing change in γH2AX staining in in early and late passage human primary endothelial cells. Early passage cell counts are shown in black, late passage cell counts are given in grey. Cell counts were obtained by manual counting of multiple fields in 6-well plates from 3 biological replicates. $N > 300$ cells for each replicate. Error bars represent standard deviation of measurement. Statistical significance was determined by one-way ANOVA with $* = p \leq 0.05$, $*** = \leq 0.001$ and $**** = p \leq 0.0001$.

demonstrating an approximate 33 % decrease in the number of cells staining positive for SA-β-Gal activity ($p = 0.0016$; Fig. 2).

3.2. miRNAs demonstrating dysregulated expression in senescence and upon resveratrol treatment

Whole miRNome profiling of early and late passage human primary endothelial cells revealed that 404 miRNAs were expressed in early and/or late passage primary human endothelial cells. Of these, 244 miRNAs demonstrated nominal significance for an association with senescence, and 202 demonstrated significance following adjustment for false discovery rate (Fig. 3; Online Resource 1). The most dysregulated miRNA

were miR-6850-5p (fold change = −38.69; FDR adjusted *p* value = 0.0002), miR-4687-3p (fold change = −29.59; FDR adjusted p value; Online Resource 1 = 0.0005), miR-7108-5p (fold change = −28.03; FDR adjusted p value = 0.0007), miR-4632-5p (fold change = −10.49; FDR adjusted p value = 0.001) and miR-4530 (fold change = −16.12; FDR adjusted p value = 0.001). We have previously demonstrated that low dose resveratrol is capable of bringing about reversal of multiple senescent cell phenotypes in human primary dermal fibroblasts (Latorre, 2017). Accordingly, treatment of late passage human primary endothelial cells also showed a rescue phenotype when treated with low dose (5 μM) resveratrol (Fig. 2). We identified 202 miRNAs were expressed in senescent primary human endothelial cells treated with resveratrol, of

Fig. 2. Senescence-associated beta galactosidase activity in late passage (PD = 84) human primary endothelial cells treated with 5 mM resveratrol for 48 h. (A) Microscope fields illustrating representative senescence-associated beta galactosidase (SA-β-Gal) activity in late passage (PD = 84) human primary endothelial cells treated with resveratrol (RSV) or with vehicle (DMSO) alone. (B) Graph showing change in SA-β-Gal activity in early and late passage human primary endothelial cells. (C) Proliferation kinetics in RSV or vehicle treated cells. stained for Ki67 activity. (D) Graph showing change in Ki67 staining in RSV or vehicle treated cells. (E) DNA damage foci as identified by γH2AX staining in RSV or vehicle treated cells. (F) Graph showing change in γH2AX staining in RSV or vehicle treated cells. Vehicle treated cells are shown in black, RSV treated cells in grey. Cell counts were obtained by manual counting of multiple fields in 6-well plates from 3 biological replicates. *N* > 400 cells for each replicate. Error bars represent standard deviation of measurement. Statistical significance was determined by one-way ANOVA with ** = ≤0.001.

which 35 demonstrated nominal associations with senescence, and 3 met multiple testing criteria (Fig. 3; Online Resource 2). These were miR-5787 (fold change −1.76; FDR adjusted *p* value = 0.0005), miR-3665 (fold change −3.36; FDR-adjusted p value = 0.001) and miR-361-5p; fold change 1.41; FDR adjusted *p* value = 0.001). The changes we identified in miR-361-5p expression we noted in our Clariom D data were also confirmed in a new culture of senescent cells by qRTPCR (Online Resource 3).

3.3. miR-361-5p demonstrates opposing differential expression in response to senescence and reversal

MiRNA differentially regulated with senescence comprise a mix of those that may induce senescence and those that are a result of it. Similarly, not all miRNA that are responsive to resveratrol will be directly involved in the reversal response, due to the pleiotropic nature of the molecule. To focus our analysis on those miRNAs which may be directly involved in the reversal response, we identified those that are present at the juxtaposition of both datasets, but with opposite direction of effect. One miRNA, miR-361-5p fulfilled these criteria (Fig. 3), demonstrating a 1.52-fold decrease in expression in senescent endothelial cells (FDR- adjusted *p* value = 0.05) and a 1.41-fold increase in expression following resveratrol treatment (FDR- adjusted p value = 0.001).

3.4. Identification of miR-361-5p target genes and assessment of their expression in senescent human primary endothelial cells

Identification of validated miR-361-5p target genes using miRTarBase version 9.0 revealed that miR-361-5p regulates 839 mRNA transcripts. Of these, we determined that 65 were expressed in human primary endothelial cells. 32 miR-361-5p target genes demonstrated an association with senescence below an Benjamini Hochberg corrected FDR *p* value threshold 0f 0.05 (Fig. 4; Online Resource 4). However, in
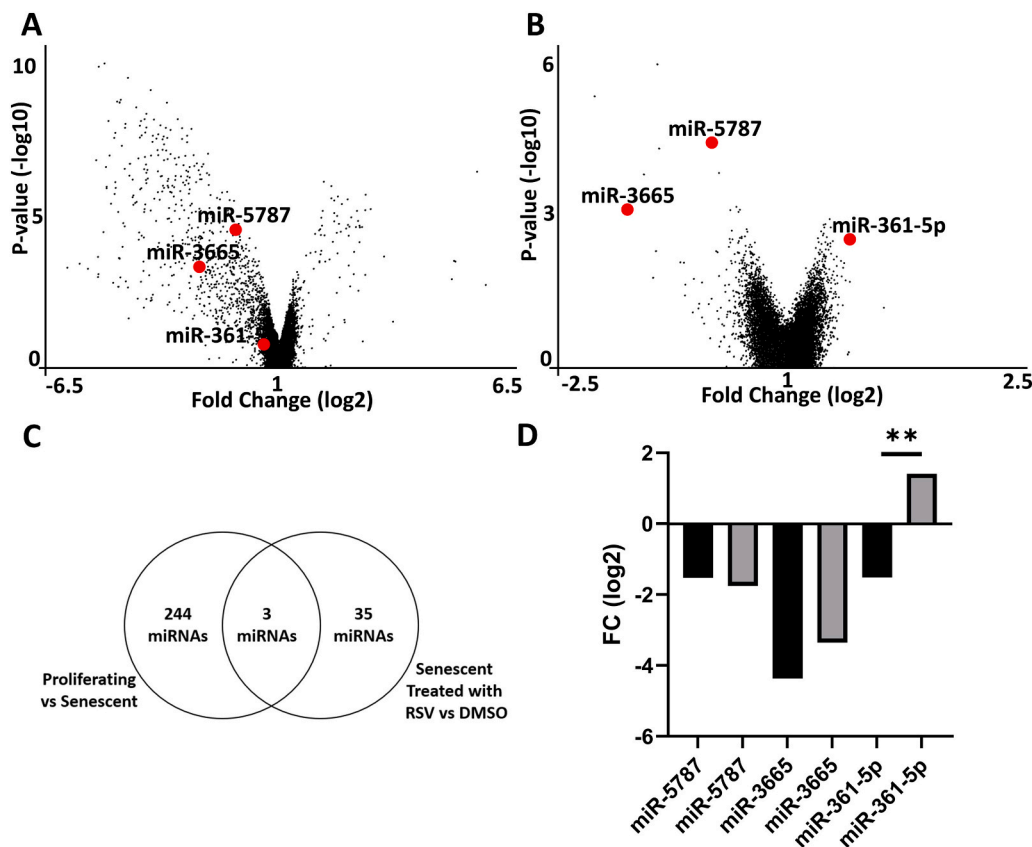
Fig. 3. Analysis of miRNAs expression profiles associated with endothelial cell senescence and rescue. (A) Volcano plot illustrating differentially-expressed miRNAs in senescent human primary endothelial cells. (B) Volcano plot illustrating differentially-expressed miRNAs in rejuvenated senescent human primary endothelial cells. (C) Venn diagram to summarize overlap between miRNA datasets differentially expressed in senescence and those differentially expressed in rejuvenation. (D) Expression pattern of miR-361-5p in senescent (black bars) and rejuvenated (grey bars) human primary endothelial cells expressed as a fold change compared with young or vehicle treated cells. Statistical significance was adjusted for multiple testing by Benjamini FDR. ** = ≤0.001.

Fig. 4. Differential expression of miR-361-5p targets in early and late passage human primary endothelial cells. The expression patterns of 35 validated miR-361-5p target genes in early (PD = 36) and late (PD – 84) passage human primary endothelial cells are given. Black bars indicate early passage cells (PD = 36), lighter grey bars indicate late passage cells (PD = 84; n = 3 biological replicates for each). The Y axis refers to relative quantification arbitrary units (AU). Error bars represent standard deviation of measurement. Statistical significance was determined by t-test and * = $p \leq 0.05$, ** = ≤0.001 and *** = $p \leq 0.0001$.

contrast to our predictions, the vast majority of miR-361-5p target genes demonstrated reduced, rather than elevated levels of expression in senescent primary endothelial cells relative to their early passage counterparts. The most dysregulated miR-361-5p target genes in senescent endothelial cells included *TMEM43* (fold change > − 1000; FDR adjusted p value = 0.002), *LPAR1* (fold change = −136.53; FDR adjusted p value = 0.003), *RECK* (fold change = −44.98; FDR adjusted p value = 0.02), *RAD23B* (fold change = −18.2; FDR adjusted p value = 0.008), *RAD23A* (fold change = −16.1; FDR adjusted p value = 0.02) and *TGFBR1* (fold change = −15.92' FDR adjusted p value = 0.006). Only *EZR* (fold change 19.35; FDR adjusted p value = 0.02) and *ARPC5* (fold change 3.92; FDR adjusted p value = 0.035) demonstrated an increase in senescent cells, which would be consistent with the most predominant mode of miRNA regulation.

3.5. Pathway analysis of restored miRNA and their target genes

We carried out a Cellular and Molecular Function and Biological Processes GO terms analysis for the target genes of the 32 miR-361-5p target genes demonstrating differential expression in senescent primary human endothelial cells (Table 1), as well as targets of other miRNA associated with senescence or reversal individually (Tables 2 and 3).

The cellular function pathways that were enriched in miR-361-5p target genes included those involved in cytoskeletal remodeling (focal adhesion; adjusted p value ≤0.0001, actin filament; adjusted p value = 0.004, polymeric cytoskeletal fiber; p = 0.008) or with the core splicing machinery with the splicing machinery (U5 snRNP; adjusted p value ≤0.0001, U4/U6 × U5 tri snRNP complex; adjusted p value = 0.008, spliceosomal tri-snRNP complex; adjusted p value 0.008, spliceosomal

Table 1

Gene Ontology (GO) cellular, molecular and biological processes enriched in senescence-associated miR-361-5p target genes in primary human endothelial cells. Adjusted *p* values have been derived from Fisher exact test for gene set enrichment in each pathway. Odds ratio refers to the probability that gene sets are enriched in a particular pathway and combined score is the Fisher exact test *p*-value multiplied by the z-score for deviation from expected rank.

Term	p value	Adj p value	Odds ratio	Combined score
GO cellular function				
Focal adhesion (GO:0005925)	0.000	<0.001	18.79	310.3
Actin filament (GO:0005884)	0.000	0.004	39.62	368.12
U5 snRNP (GO:0005682)	0.001	0.008	63.32	468.27
U4/U6 × U5 tri-snRNP complex (GO:0046540)	0.001	0.008	57.81	417.77
Golgi lumen (GO:0005796)	0.001	0.008	21.64	164.04
Spliceosomal complex (GO:0005681)	0.001	0.008	18.51	132.13
Polymeric cytoskeletal fiber (GO:0099513)	0.000	0.008	13	101.44
Spliceosomal tri-snRNP complex (GO:0097526)	0.001	0.010	45.84	311.42
Spliceosomal snRNP complex (GO:0097525)	0.004	0.024	23.29	128.53
Filopodium (GO:0030175)	0.004	0.024	22.89	125.56
Ficolin-1-rich granule membrane (GO:0101003)	0.004	0.024	22.5	122.69
Platelet alpha granule lumen (GO:0031093)	0.005	0.025	20.41	107.6
Endocytic patch (GO:0061645)	0.011	0.043	107.32	482.58
Actin cortical patch (GO:0030479)	0.011	0.043	107.32	482.58
GO molecular function				
Polyubiquitin modification-dependent protein binding (GO:0031593)	0.000	0.001	51.54	517.04
Ubiquitin-specific protease binding (GO:1990381)	0.000	0.006	95.02	772.86
Protein kinase A regulatory subunit binding (GO:0034237)	0.000	0.006	83.13	656.15
Disordered domain specific binding (GO:0097718)	0.001	0.009	63.32	468.27
GO biological processes				
Regulation of cellular component movement (GO:0051270)	0.000	0.001	67.78	948.18
Positive regulation of cellular component movement (GO:0051272)	0.000	0.002	114.66	1402.93
Positive regulation of stress fiber assembly (GO:0051496)	0.000	0.004	60.65	636.13
Vesicle transport along actin filament (GO:0030050)	0.000	0.004	266.17	2626.53
Cytoskeletal anchoring at plasma membrane (GO:0007016)	0.000	0.006	190.1	1773.82
Actin filament-based transport (GO:0099515)	0.000	0.007	166.33	1515.06
Negative regulation of DNA damage response, signal transduction by p53 class mediator (GO:0043518)	0.000	0.008	133.05	1161.23
Embryonic cranial skeleton morphogenesis (GO:0048701)	0.000	0.011	102.33	845.92
Negative regulation of signal transduction by p53 class mediator (GO:1901797)	0.000	0.011	102.33	845.92
Cardiac epithelial to mesenchymal transition (GO:0060317)	0.000	0.011	95.02	772.86

Table 2

Gene Ontology (GO) cellular, molecular and biological processes enriched in late passage primary human endothelial cells compared to early passage cells. The top ten pathways are given for each GO category. Adjusted p values have been derived from Fisher exact test for gene set enrichment in each pathway. Odds ratio refers to the probability that gene sets are enriched in a particular pathway and combined score is the Fisher exact test p-value multiplied by the z-score for deviation from expected rank.

Term	P-value	Adjusted P-value	Odds ratio	Combined score
GO cellular function				
Integral component of nuclear inner membrane (GO:0005639)	0.006	0.386	20.20	103.22
Intrinsic component of nuclear inner membrane (GO:0031229)	0.006	0.386	20.20	103.22
GO molecular function				
Small GTPase binding (GO:0031267)	0.002	0.150	4.28	27.00
RNA polymerase II transcription regulatory region sequence-specific DNA binding (GO:0000977)	0.0022	0.150	2.00	12.40
GTPase regulator activity (GO:0030695)	0.0022	0.150	3.66	22.25
RNA polymerase II cis-regulatory region sequence-specific DNA binding (GO:0000978)	0.0022	0.150	2.07	12.55
GTPase binding (GO:0051020)	0.004	0.150	3.70	20.49
Ubiquitination-like modification-dependent protein binding (GO:0140035)	0.004	0.150	25.25	138.38
Cis-regulatory region sequence-specific DNA binding (GO:0000987)	0.005	0.150	1.97	10.40
Mitogen-activated protein kinase kinase kinase binding (GO:0031435)	0.005	0.150	22.44	118.64
Ubiquitin-dependent protein binding (GO:0140036)	0.005	0.150	22.44	118.64
GTPase activator activity (GO:0005096)	0.006	0.172	2.84	14.30
GO biological processes				
Positive regulation of neurogenesis (GO:0050769)	0.000	0.303	7.63	55.02
Positive regulation of dendrite morphogenesis (GO:0050775)	0.000	0.303	17.90	124.35
Negative regulation of catabolic process (GO:0009895)	0.001	0.303	9.052	59.53
Cholesterol import (GO:0070508)	0.001	0.303	50.51	330.99
Sterol import (GO:0035376)	0.001	0.303	50.51	330.99
Bleb assembly (GO:0032060)	0.002	0.303	40.40	251.45
Regulation of transcription, DNA-templated (GO:0006355)	0.002	0.303	1.77	10.70
Aspartate family amino acid biosynthetic process (GO:0009067)	0.003	0.303	33.67	200.06
Regulation of microvillus organization (GO:0032530)	0.003	0.303	33.67	200.06
Sulfur amino acid biosynthetic process (GO:0000097)	0.003	0.303	33.67	200.06

complex; adjusted p value = 0.004). Molecular processes enriched in miR-361-5p target genes included processes involved in ubiquitination (polyubiquitin modification-dependent protein binding; adjusted p value = 0.001, and ubiquitin-specific protease binding; adjusted p value = 0.006). Biological processes enriched on miR-361-5p target genes

included those involved in movement of cellular cargoes (cellular component movement; adjusted p value = 0.001, positive regulation of cellular component movement; adjusted p value = 0.002, vesicle transport along actin filaments; adjusted p value = 0.004) and stress

Table 3

Gene Ontology (GO) cellular, molecular and biological processes enriched in in primary human endothelial cells in response to resveratrol treatment. Adjusted p values have been derived from Fisher exact test for gene set enrichment in each pathway. Odds ratio refers to the probability that gene sets are enriched in a particular pathway and combined score is the Fisher exact test p-value multiplied by the z-score for deviation from expected rank.

	p value	Adj p value	Odds ratio	Combined score
GO cellular function				
Cytoskeleton (GO:0005856)	0.000	0.031	4.530	35.90
GO molecular function				
Ubiquitin-dependent protein binding (GO:0140036)	0.000	0.056	61.472	444.24
Cholesterol transfer activity (GO:0120020)	0.002	0.056	34.566	215.01
Sterol transfer activity (GO:0120015)	0.002	0.05	32.531	198.81
DNA-binding transcription repressor activity, RNA polymerase II-specific (GO:0001227)	0.003	0.056	5.680	33.82
Ubiquitin protein ligase activity (GO:0061630)	0.003	0.056	5.524	32.25
Ubiquitin-like protein ligase activity (GO:0061659)	0.003	0.056	5.376	30.78
Ubiquitin-protein transferase activity (GO:0004842)	0.003	0.056	4.467	25.53
GO biological processes				
Negative regulation of transcription by RNA polymerase II (GO:0000122)	0.000	0.030	4.995	50.50
Negative regulation of transcription, DNA-templated (GO:0045892)	0.000	0.065	3.927	33.98
T cell apoptotic process (GO:0070231)	0.000	0.070	110.672	905.29
Positive regulation of transcription by RNA polymerase II (GO:0045944)	0.000	0.090	3.704	28.27
Regulation of transcription by RNA polymerase II (GO:0006357)	0.000	0.135	2.606	18.21
Aorta development (GO:0035904)	0.001	0.135	46.097	310.25
Positive regulation of transcription, DNA-templated (GO:0045893)	0.001	0.135	3.100	20.69
Aorta morphogenesis (GO:0035909)	0.002	0.135	36.872	233.61
Histone H2A ubiquitination (GO:0033522)	0.0024	0.135	36.872	233.61
Peptidyl-threonine modification (GO:0018210)	0.002	0.135	13.113	81.72

granule formation (positive regulation of stress fiber assembly; adjusted p value = 0.004). Data are presented in Table 1.

We then assessed Cellular and Molecular Function and Biological Processes pathway enrichment for targets of the top 10 miRNAs demonstrating associations with senescence. Molecular function pathways demonstrating nominal enrichment were those involved in signal transduction (small GTPase binding; GO:0031267), GTPase regulator activity; GO:0030695), transcription (RNA polymerase II transcription regulatory region sequence-specific DNA binding; GO:0000977, RNA polymerase II cis-regulatory region sequence-specific DNA binding; GO:0000978), ubiquitination (ubiquitination-like modification-dependent protein binding; GO:0140035, ubiquitin-dependent protein binding; GO:0140036) and MAPK signaling (mitogen-activated protein kinase kinase kinase binding; GO:0031435), although none passed an FDR-adjusted significance threshold (Table 2). Targets of resveratrol-

associated mRNAs were enriched in biological process pathways involved in regulation of transcription (negative regulation of transcription by RNA polymerase II; FDR adjusted p value = 0.03), whilst cellular function pathways enriched in resveratrol-regulated miRNAs were involved in the regulation of the cytoskeleton (cytoskeleton; FDR adjusted p value = 0.03; Table 3). All 3 resveratrol-associated miRNAs were also associated with senescence.

3.6. Restoration of miR-361-5p levels in aged cells causes a decrease in SA-β-Gal positive cells

To determine whether miR-361-5p influences cellular senescence phenotypes, we treated primary senescent human endothelial cells with miR-361-5p mimic. Transfection efficiencies were > 90 % and miR-361-5p levels were restored to those comparable with early passage cells. We identified that increasing levels of miR-361-5p in aged endothelial cells resulted in an approximately 14 % drop in the percentage of senescent cells in the culture (the percentage of senescent cells in cells treated with carrier only was 52 % (SD = 8 %) compared with 38 % (SD = 7 %) in mimic treated cells; p = 0.013; Fig. 5). We noted no differences in proliferation index (as measured by Ki67) or the number of DNA damage foci (measured by γH2AX), indicating that the reversal effect was only partial.

3.7. miR-361-5p target genes do not promote lifespan and healthspan phenotypes in C. elegans

We next sought to determine whether RNAi knockdown of the worm orthologues of the 16 C. elegans orthologues of validated miR-361-5p target genes with differential expression in senescent human endothelial cells were associated with altered lifespan or healthspan parameters in vivo. A miRNA demonstrating down-regulation in aged cells would be expected to lead to up-regulation of its target genes, if it is the predominant regulatory factor. Of the 16 genes tested however, only 2 (erm-1/EZR and C46H11.3/ARPC5L) demonstrated elevated expression in senescent primary endothelial cells, whereas the remainder demonstrated reduced levels of expression. However, since miRNAs have been known to positively regulate target genes under some circumstances (Cheng et al., 2021; Hong et al., 2020), we elected to also assess the effect of targeted knockdown of all 16 miR361-5p target genes with worm orthologues in our C. elegans work. Of the 16 orthologues tested, 9/16 demonstrated effects on lifespan and 12/16 demonstrated effects on healthspan, as assessed by movement rate across the ageing trajectory. However, in all cases, targeted knockdown was associated with an adverse outcome for both measures; reduction in target gene expression was associated with decreased, not increased, lifespan and healthspan (Fig. 6).

4. Discussion

MicroRNAs are key components of the cellular stress response and are pivotal to a multitude of cellular processes. Here, we report the miRNA profiles associated with cellular senescence and those associated with polyphenol-induced rescue from senescence, in human primary endothelial cells. We have identified one miRNA, miR-361-5p, which demonstrates antagonistic patterns of expression in response to senescence and rejuvenation. GO terms analysis reveals that validated targets of this miRNA are enriched in pathways involved in transport of materials and cellular components in the cytosol by actin filaments and vesicles, and with components of the core spliceosome. Manipulation of miR-361-5p levels using a miRNA mimic resulted in a reduction of the senescent cell load in aged primary endothelial cells. In contrast with these findings however, targeted knockdown of validated miR-361-5p target genes in an invertebrate model animal C. elegans was not associated with increased lifespan and healthspan, indeed knockdown of these genes was detrimental. From this we conclude that although miR-361-
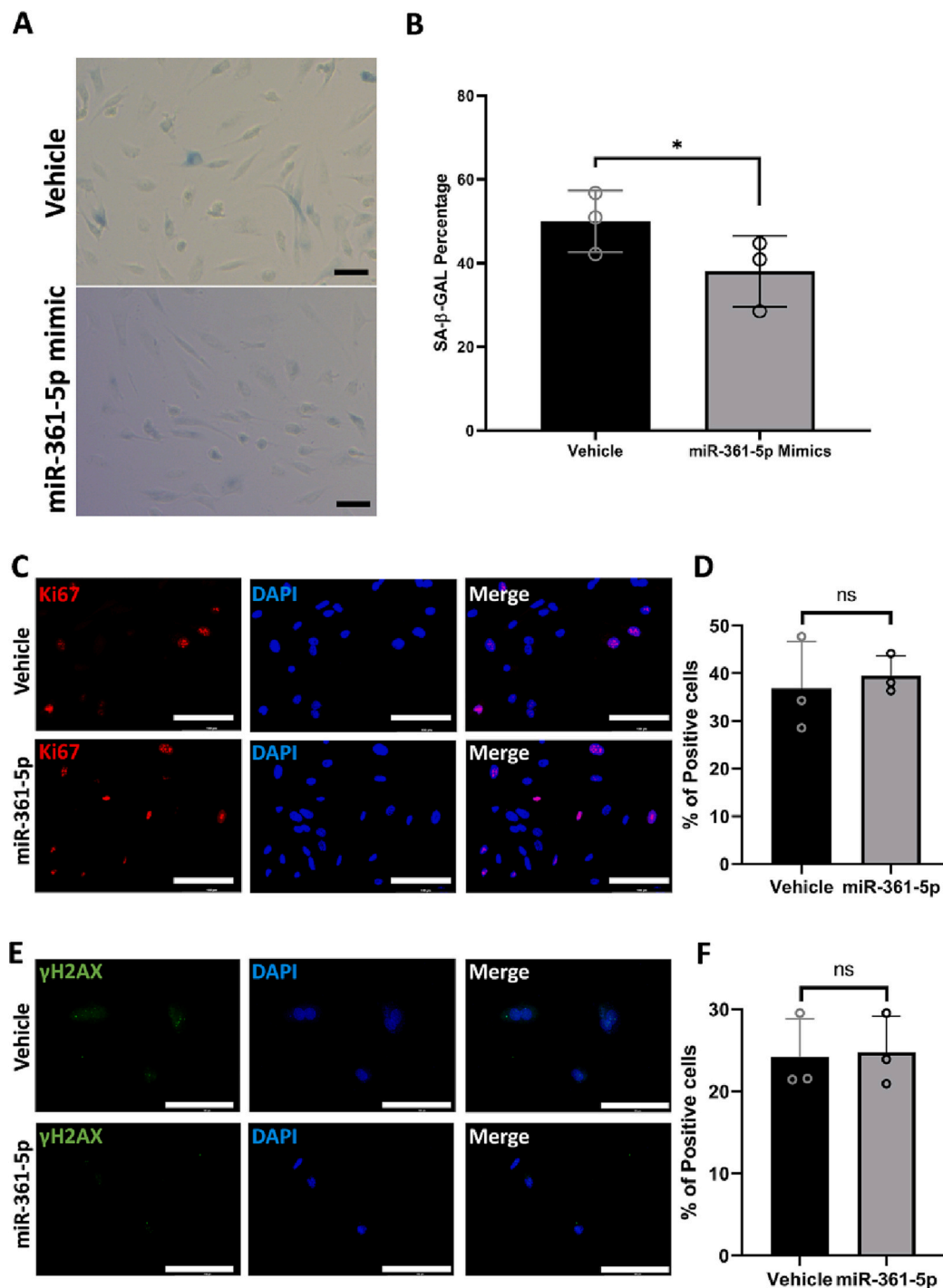
Fig. 5. Attenuation of cellular senescence in aged endothelial cells using a mimic to miR-361-5p. (A) Microscope fields illustrating representative senescence-associated beta galactosidase (SA-β-Gal) activity in late passage (PD = 84) human primary endothelial cells treated with a miR-361-5p mimic or with vehicle alone. (B) Graph showing change in SA-β-Gal activity in mimic or vehicle treated cells. (C) Proliferation kinetics in mimic or vehicle treated cells. stained for Ki67 activity. (D) Graph showing change in Ki67 staining in mimic or vehicle treated cells. (E) DNA damage foci as identified by γH2AX staining in mimic or vehicle treated cells. (F) Graph showing change in γH2AX staining in mimic or vehicle treated cells. (The black bars represent senescent cell load in vehicle treated cells, whilst the grey bars represent senescent cell load following treatment with a miR-361-5p mimic. Transfection efficiency was >90 %. Error bars indicate standard deviation of measurement. Statistical significance of effect as determined by independent t-test is indicated by a star * ≤0.05.

5p may contribute to aspects of the senescent cell phenotype, targeted manipulation of it alone is not likely to bring about beneficial effects in systems.

Altered expression of miR-361-5p has previously been associated with multiple diseases with an age-related component in multiple tissue types. These include acute coronary syndrome and coronary artery disease (Su et al., 2020), osteoarthritis (Wang et al., 2019), rheumatoid arthritis (Romo-Garcia et al., 2019), hepatic steatosis (Zhang et al., 2018), hypertension (Qi et al., 2017), Alzheimer's disease (Mendes-Silva et al., 2016) and macular degeneration (Grassmann et al., 2014). MicroRNA miR-361-5p also has known roles in epithelial-to-mesenchymal cell transition (Yin et al., 2020; Zhang et al., 2017; Wu

et al., 2013) which may underpin its associations with the development or progression of multiple cancers, including those of the reproductive (Ling and He, 2021; Zheng et al., 2021; Yang and Xie, 2020), respiratory (Othman and Nagoor, 2019; Zhuang et al., 2016), digestive (Qian et al., 2020; Cui et al., 2016), skeletal (Shen et al., 2019) and nervous systems (Zhou et al., 2020). We identified that the expression of miR-361-5p was decreased in human primary endothelial cells, but upregulated in these cells in response to treatment with a polyphenol small molecule associated with cellular rejuvenation in our previous work (Latorre, 2017). Targeted upregulation of miR-361-5p was able to attenuate some aspects of senescence in senescent endothelial cells. This suggests that miR-361-5p may be contributory to the establishment or maintenance of
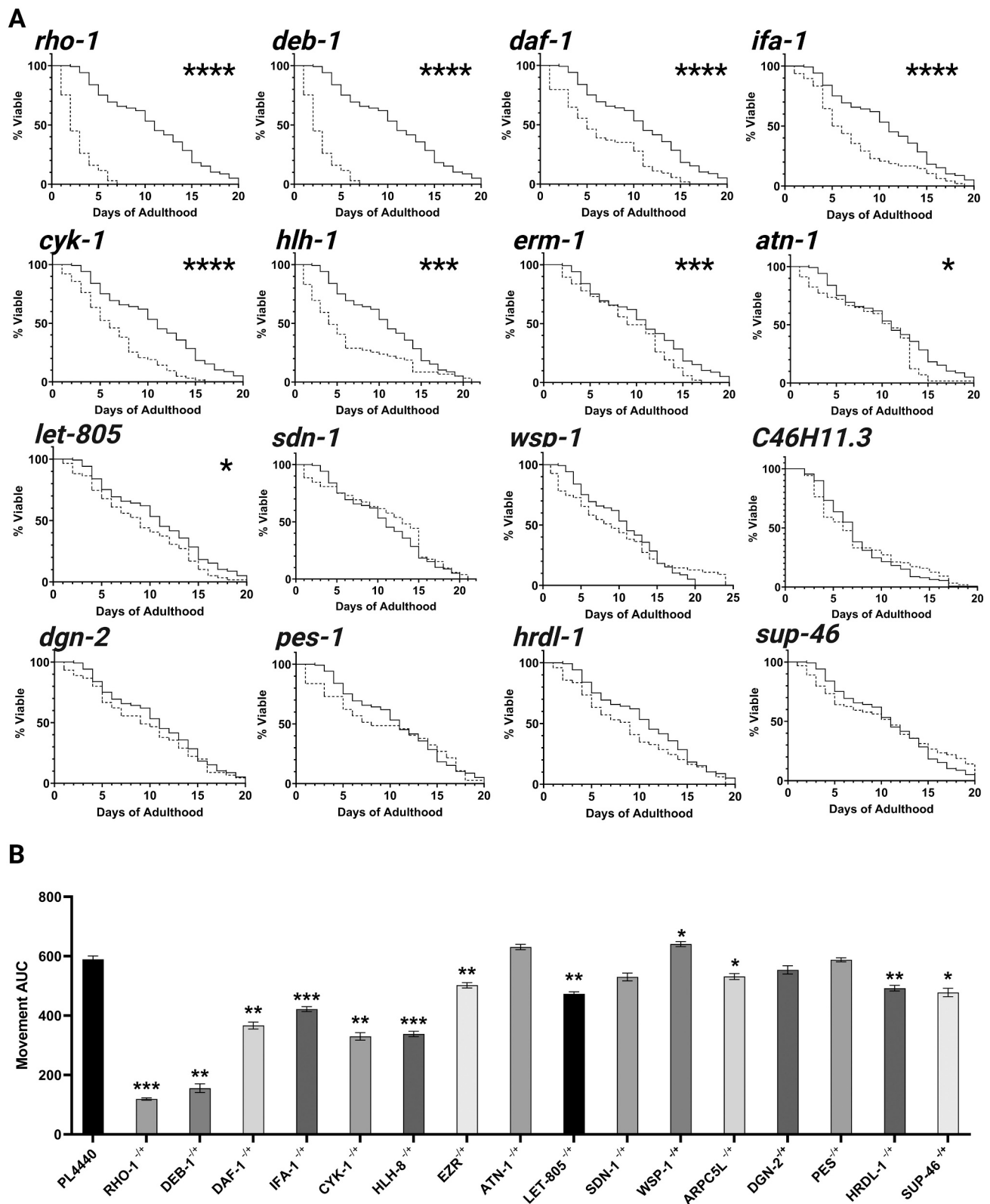
Fig. 6. Attenuation of miR-361-5p target genes in a *C. elegans* model system. **A.** Survival curves illustrating the effect of targeted RNAi knockdown of 16 validated miR-361-5p target genes with known *C. elegans* orthologues. Probability of survival is given on the Y axis and days from start of analysis is given on the X axis. Data from control animals is given by solid black lines, data from treated animals is given by dashed grey lines. **B.** Area under the curve (AUC) measurements for a measure of healthspan (animal movement) following targeted RNAi knockdown of 16 validated miR-361-5p target genes with known *C. elegans* orthologues are given on the Y axis, and the identity of the gene on the X axis. Error bars represent standard deviation of measurement. In each case, data are from 3 biological replicates of 60–70 animals per replicate. $* = p \leq 0.05$, $** = \leq 0.01$, $*** = p \leq 0.001$ and $**** = p \leq 0.0001$.

some aspects of the senescent cell phenotype in endothelial cells.

It is important to note also that senescence is a collection of phenotypes, which are not always coordinately-regulated and it is possible to uncouple these aspects in a cell-type and intervention-specific manner. We have previously demonstrated that attenuation of human primary endothelial cell senescence in the absence of re-entry to cell cycle following treatment with the endogenous gasotransmitter H₂S (Latorre et al., 2018). It is possible that different aspects of the senescent cell phenotype may be regulated by different factors, and that treatment with a miR-361-5p mimic may attenuate some, but not all, of these factors.

Targeted manipulation of validated miR-361-5p target genes in a *C. elegans* animal model was however not able to extend lifespan or healthspan parameters systemically when manipulated in adulthood. Although *C. elegans* do not undergo replicative senescence in the conventional sense due to the post-mitotic nature of their adult somatic cells, they do undergo other forms of senescence (Benedetto and Gems, 2019). Interventions designed to attenuate senescence phenotypes therefore have potential to extend healthspan and lifespan in this system. We identified two target genes (*erm-1/EZR* and *C46H11.3/ARPC5L*) that demonstrated up-regulation of expression, consistent with the action of a down-regulated miRNA in senescence. The direction of change for most of the other miR-361-5p targets observed in senescent primary human endothelial cells however was inconsistent with the proposed action of a miRNA; the majority of validated targets demonstrated reduced rather than elevated expression in senescent cells. Although there are examples where miRNA can upregulate their targets in the context of senescence (Hong et al., 2020), this probably indicates that the majority of miR-361-5p targets are regulated by factors other than miR-361-5p in senescence.

Many of the validated target genes of miR-361-5p have known roles in senescence or ageing. Genetic variation in the *TMEM43* gene has been associated with longevity in the Chinese population (Liu et al., 2021), whereas transcript levels of *HNRNPM* are predictive of ageing phenotypes in human peripheral blood mRNA (Lee et al., 2019). Pharmacological reduction of *LPAR1* expression has been associated with induction of senescence in HuH7 cells in vitro via modulation of the cytoskeleton (PMID (Konopa et al., 2022)). *TGFB1* is known to be a component of the senescence associated secretory phenotype (SASP) but is also a known provocation for senescence in its own right (Zhang et al., 2020). Reduced expression of *RAD23B, ZMAT3* and *IQGAP1* expression has been reported to induce senescence in human diploid fibroblasts (Comegna et al., 2014), pre-adipocytes (Spinelli et al., 2022) and vascular smooth muscle cells (Grabowska et al., 2020) respectively. Similarly, *TWIST1* has been shown to control senescence in mesenchymal stem cells (Voskamp et al., 2021). *WASL*, which encodes N-WASP, is an inhibitor of p53 induced senescence (Li et al., 2019). *DIAPH1* is the intracellular binding effector molecule of the RAGE pathway, well known to be implicated in inflammaging and chronic disease (Ramasamy et al., 2016). Probably the best known example of miR-361-5p target gene implicated in senescence however, is the *MDM2* gene which encodes a key component of the p53 axis, with multiple roles in senescence and ageing (Wu and Prives, 2018).

It is likely however, that the miR-361-5p-regulated genes involved in attenuation of senescence responses we observe would demonstrate elevated, rather than reduced, expression in senescent cells in response to reduced miR-361-5p levels, and down-regulation in response to a miR-361-5p mimic. Of the miR-361-5p target genes expressed in human endothelial cells, only 2 (*EZR* and *ARPC5L*) demonstrated elevated expression in senescent cells and only *EZR* in a direction that would be consistent with rescue upon miR_361-5p mediated rescue. *EZR* encodes Ezrin, an actin binding protein which acts downstream of RB1 and is known to be involved in the morphological changes accompanying senescence (Yang and Hinds, 2003). Increased phosphorylation of Ezrin by CDK5 results in disassociation of the Rho GDP disassociation inhibitor (Rho-GDI) and increases the inhibitory interaction of Ezrin with the

Rac1 GTPase yielding the characteristic 'flat' morphology of senescent cells (Yang and Hinds, 2006). Despite this, we did not observe systemic improvement in healthspan or lifespan following targeted RNAi knockdown of the *C. elegans* orthologue of *EZR* (*erm-1*).

Of the remaining validated *C. elegans* ortholog of the validated miR-361-5p target genes identified, 13 are directly involved in the regulation or formation of the cytoskeletal network, or its interaction with the extracellular matrix. *rho-1/RHOA, sdn-1/SDC4, wsp-1/WASL, pes-7/IQGAP1*, and *hrdl-1/AMFR* are involved in transducing signals from the exterior of the cell to the interior to regulate cell motility, morphology and survival (Kempers et al., 2021; Elfenbein and Simons, 2013; Choi and Anderson, 2016; Dart et al., 2012; Chiu et al., 2008). *Deb-1/VCL, ifa-1/VIM, cyk-1D/IAPH1, C46H11.3/ARPC5L, hlh-8/TWIST1* and *atn-1/ACTN4* are involved with formation or regulation of microtubules, intermediate filaments or other cytoskeletal components to facilitate cell attachment, cell:cell or cell:matrix interactions and EMT (Boujemaa-Paterski et al., 2020; Yang et al., 2021; Schneider et al., 2022; Hsu et al., 2022; Tentler et al., 2019; Garcia-Palmero et al., 2016). *let-805/FN1* and *dgn-2/DAG1* are extracellular matrix glycoproteins involved in cell adhesion, migration and survival (Barresi and Campbell, 2006; Owens and Baralle, 1986). The cytoskeleton and the actin filament network is widely known to regulate many aspects of cellular behaviour, particularly in the nervous system (Schneider et al., 2022), and has known involvement in the ageing process and its diseases (Kim et al., 2022). The remaining two miR-361-5p target genes we assessed sup-*46/HNRNPM* and *daf-1/TGFBR1* are also known to have associations with ageing and senescence. *TGFBR1* is part of the TGF signaling network and a major inducer of cell cycle arrest and senescence (Vander Ark et al., 2018). *HNRNPM* is a member of a gene family encoding multifunctional proteins involved in alternative splicing and other aspects of mRNA processing (Geuens et al., 2016). Dysregulation of mRNA processing has been suggested as a new hallmark of ageing (Schmauck-Medina et al., 2022), and dysregulation of *HNRNPM* expression has been associated with ageing, senescence and age-related phenotypes in humans and other species (Latorre, 2017; Lee et al., 2019; Lee et al., 2016). It is possible that the partial attenuation of the senescent cell phenotype we have described in response to elevation of miR-361-5p levels is due to consequent reduction in the expression of other genes that we have not assessed, but without knowledge of the identity of those target genes, and very specific approaches to influence their interaction with this miR, miR-361-5p is unlikely to represent an immediate and tractable senotherapeutic target.

It is also possible that the miRNA:target dynamic may be divergent between humans and *C. elegans*. Although microRNA are usually conserved at the seed sequence level across species (de Wit et al., 2009), they do appear to have higher rates of evolutionary divergence than do other types of genes (Mao et al., 2014), and species-specific mRNAs have been reported in plants (Guo et al., 2022). More likely however are differences in the target gene repertoire between man and *C. elegans*. miRNA binding sites are short and degenerate and are usually sited in the 3′ untranslated region of transcripts, which are under less evolutionary constraint than the coding regions. As such, miRNA sites present in one species may be absent in another (Mor and Shomron, 2013).

5. Conclusions

In conclusion, we report here the identification of a miRNA (miR-361-5p) that displays antagonistic effects in cellular senescence and cellular rejuvenation in human primary endothelial cells. We have validated its predicted target genes and demonstrated that several display dysregulated expression in senescent primary human endothelial cells. Although targeted manipulation of miR-361-5p was able to bring about reversal of some aspects of the senescence phenotype in human primary endothelial cells in vitro, many of its target genes are also involved in critical cellular processes. A more nuanced approach to the potential therapeutic potential of modulating miR-361-5p may be to

specifically target its interaction with those targets that are drivers of senescence but not critical to cellular function.

Credit authorship contribution statement

Conceptualization, Lorna Harries; Data curation, Lorna Harries and Emad Manni; Formal analysis, Emad Manni, Nicola Jeffery, David Chambers, Luke Slade and Lorna Harries; Investigation, Emad Manni, Luke Slade and David Chambers; Methodology, Emad Manni; Project administration, Lorna Harries; Resources, Lorna Harries; Supervision, Nicola Jeffery, Tim Etheridge and Lorna Harries, draft, Emad Manni; Writing – review & editing, Nicola Jeffery, David Chambers, Luke Slade, Tim Etheridge and Lorna Harries.

Competing interests

LWH holds a position as Co-founder, Co-director and CSO of SENISCA Ltd.

Data availability

The data presented in this study are available upon reasonable request from the corresponding author. The data are not publicly available for reasons of intellectual property.

Acknowledgments

Appendix A. Supplementary data

Supplementary data to this article can be found online at https://doi.org/10.1016/j.exger.2023.112127.

References

Baker, D.J., et al., 2011. Clearance of p16Ink4a-positive senescent cells delays ageing-associated disorders. Nature 479 (7372), 232–236.

Baker, D.J., et al., 2016. Naturally occurring p16(Ink4a)-positive cells shorten healthy lifespan. Nature 530 (7589), 184–189.

Barresi, R., Campbell, K.P., 2006. Dystroglycan: from biosynthesis to pathogenesis of human disease. J. Cell Sci. 119 (Pt 2), 199–207.

Bartel, D.P., 2004. MicroRNAs: genomics, biogenesis, mechanism, and function. Cell 116 (2), 281–297.

Benedetto, A., Gems, D., 2019. Autophagy promotes visceral aging in wild-type C. Elegans. Autophagy 15 (4), 731–732.

Boujemaa-Paterski, R., et al., 2020. Talin-activated vinculin interacts with branched actin networks to initiate bundles. elife 9.

Brenner, S., 1974. The genetics of Caenorhabditis elegans. Genetics 77 (1), 71–94.

Bussian, T.J., et al., 2018. Clearance of senescent glial cells prevents tau-dependent pathology and cognitive decline. Nature 562 (7728), 578–582.

Chakraborty, C., et al., 2017. Therapeutic miRNA and siRNA: moving from bench to clinic as next generation medicine. Mol. Ther.–Nucleic Acids 8, 132–143.

Chen, E.Y., et al., 2013. Enrichr: interactive and collaborative HTML5 gene list enrichment analysis tool. BMC Bioinformatics 14, 128.

Chen, Y.L., et al., 2020. MicroRNA-214 modulates the senescence of vascular smooth muscle cells in carotid artery stenosis. Mol. Med. 26 (1), 46.

Cheng, H.P., et al., 2021. MicroRNA-362 negatively and positively regulates SMAD4 expression in TGF-beta/SMAD signaling to suppress cell migration and invasion. Int. J. Med. Sci. 18 (8), 1798–1809.

Childs, B.G., et al., 2017. Senescent cells: an emerging target for diseases of ageing. Nat. Rev. Drug Discov. 16 (10), 718–735.

Chiu, C.G., et al., 2008. Autocrine motility factor receptor: a clinical review. Expert. Rev. Anticancer. Ther. 8 (2), 207–217.

Choi, S., Anderson, R.A., 2016. IQGAP1 is a phosphoinositide effector and kinase scaffold. Adv. Biol. Regul. 60, 29–35.

Comegna, M., et al., 2014. Identification of miR-494 direct targets involved in senescence of human diploid fibroblasts. FASEB J. 28 (8), 3720–3733.

Cui, W., et al., 2016. miR-361-5p inhibits hepatocellular carcinoma cell proliferation and invasion by targeting VEGFA. Biochem. Biophys. Res. Commun. 479 (4), 901–906.

Dart, A.E., et al., 2012. Nck and Cdc42 co-operate to recruit N-WASP to promote FcgammaR-mediated phagocytosis. J. Cell Sci. 125 (Pt 12), 2825–2830.

Du, J., et al., 2019. The critical role of microRNAs in stress response: therapeutic prospect and limitation. Pharmacol. Res. 142, 294–302.

Elfenbein, A., Simons, M., 2013. Syndecan-4 signaling at a glance. J. Cell Sci. 126 (Pt 17), 3799–3804.

Ellwood, R.A., et al., 2021. Mitochondrial hydrogen sulfide supplementation improves health in the C. Elegans duchenne muscular dystrophy model. Proc. Natl. Acad. Sci. U. S. A. 118 (9).

Fougere, B., et al., 2017. Chronic inflammation: accelerator of biological aging. J. Gerontol. A Biol. Sci. Med. Sci. 72 (9), 1218–1225.

Garcia-Palmero, I., et al., 2016. Twist1-induced activation of human fibroblasts promotes matrix stiffness by upregulating palladin and collagen alpha1(VI). Oncogene 35 (40), 5224–5236.

Geuens, T., Bouhy, D., Timmerman, V., 2016. The hnRNP family: insights into their role in health and disease. Hum. Genet. 135 (8), 851–867.

Grabowska, W., et al., 2020. IQGAP1-dysfunction leads to induction of senescence in human vascular smooth muscle cells. Mech. Ageing Dev. 190, 111295.

Grassmann, F., et al., 2014. A circulating microrna profile is associated with late-stage neovascular age-related macular degeneration. PLoS One 9 (9), e107461.

Grillari, J., Hackl, M., Grillari-Voglauer, R., 2010. miR-17-92 cluster: ups and downs in cancer and aging. Biogerontology 11 (4), 501–506.

Guo, Z., et al., 2022. Identification of species-specific MicroRNAs provides insights into dynamic evolution of MicroRNAs in plants. Int. J. Mol. Sci. 23 (22).

He, S., Sharpless, N.E., 2017. Senescence in health and disease. Cell 169 (6), 1000–1011.

Holly, A.C., et al., 2013. Changes in splicing factor expression are associated with advancing age in man. Mech. Ageing Dev. 134 (9), 356–366.

Hong, Y., et al., 2020. miR-155-5p inhibition rejuvenates aged mesenchymal stem cells and enhances cardioprotection following infarction. Aging Cell 19 (4), e13128.

Hsu, P.H., et al., 2022. Skin proteomic profiling of irradiation-induced fibrosis and its modulation by low molecular weight fucoidan via tight junction pathway. Biomed. Pharmacother. 153, 113417.

Huang, H.Y., et al., 2020. miRTarBase 2020: updates to the experimentally validated microRNA-target interaction database. Nucleic Acids Res. 48 (D1), D148–D154.

Huang, H.Y., et al., 2022. miRTarBase update 2022: an informative resource for experimentally validated miRNA-target interactions. Nucleic Acids Res. 50 (D1), D222–D230.

Justice, J.N., et al., 2019. Senolytics in idiopathic pulmonary fibrosis: results from a first-in-human, open-label, pilot study. EBioMedicine 40, 554–563.

Kamath, R.S., Ahringer, J., 2003. Genome-wide RNAi screening in Caenorhabditis elegans. Methods 30 (4), 313–321.

Kempers, L., et al., 2021. The RhoGEF trio: a protein with a wide range of functions in the vascular endothelium. Int. J. Mol. Sci. 22 (18).

Kenessary, A., et al., 2013. Biomarkers, interventions and healthy ageing. New Biotechnol. 30 (4), 373–377.

Kim, W., et al., 2018. OrthoList 2: a new comparative genomic analysis of human and Caenorhabditis elegans genes. Genetics 210 (2), 445–461.

Kim, Y.J., et al., 2022. Links of cytoskeletal integrity with disease and aging. Cells 11 (18).

Konopa, A., et al., 2022. LPA receptor 1 (LPAR1) is a novel interaction partner of filamin a that promotes filamin a phosphorylation, MRTF-A transcriptional activity and oncogene-induced senescence. Oncogenesis 11 (1), 69.

LaPierre, M.P., Stoffel, M., 2017. MicroRNAs as stress regulators in pancreatic beta cells and diabetes. Mol. Metab 6 (9), 1010–1023.

Latorre, E., 2017. Small molecule modulation of splicing factor expression is associated with rescue from cellular senescence. BMC Cell Biol. 18 (1), 31.

Latorre, E., 2018. Mitochondria-targeted hydrogen sulfide attenuates endothelial senescence by selective induction of splicing factors HNRNPD and SRSF2. Aging (Albany NY) 10 (7), 1666–1681.

Lee, B.P., et al., 2016. Changes in the expression of splicing factor transcripts and variations in alternative splicing are associated with lifespan in mice and humans. Aging Cell 15 (5), 903–913.

Lee, B.P., et al., 2019. The transcript expression levels of HNRNPM, HNRNPA0 and AKAP17A splicing factors may be predictively associated with ageing phenotypes in human peripheral blood. Biogerontology 20 (5), 649–663.

Li, H., et al., 2019. Negative regulation of p53-induced senescence by N-WASP is crucial for DMBA/TPA-induced skin tumor formation. Cancer Res. 79 (9), 2167–2181.

Li, T., et al., 2016. The comparison of microRNA profile of the dermis between the young and elderly. J. Dermatol. Sci. 82 (2), 75–83.

Ling, J., He, P., 2021. miR-361-5p regulates ovarian cancer cell proliferation and apoptosis by targeting TRAF3. Exp. Ther. Med. 21 (3), 199.

Liu, X., et al., 2021. Integrated genetic analyses revealed novel human longevity loci and reduced risks of multiple diseases in a cohort study of 15,651 chinese individuals. Aging Cell 20 (3), e13323.

Lopez-Otin, C., et al., 2013. The hallmarks of aging. Cell 153 (6), 1194–1217.

Mao, X., Li, L., Cao, Y., 2014. Evolutionary comparisons of miRNA regulation system in six model organisms. Genetica 142 (1), 109–118.

Mendes-Silva, A.P., et al., 2016. Shared biologic pathways between alzheimer disease and major depression: a systematic review of MicroRNA expression studies. Am. J. Geriatr. Psychiatry 24 (10), 903–912.

Mor, E., Shomron, N., 2013. Species-specific microRNA regulation influences phenotypic variability: perspectives on species-specific microRNA regulation. Bioessays 35 (10), 881–888.

Ogrodnik, M., et al., 2017. Cellular senescence drives age-dependent hepatic steatosis. Nat. Commun. 8, 15691.

Othman, N., Nagoor, N.H., 2019. Overexpression of miR3615p plays an oncogenic role in human lung adenocarcinoma through the regulation of SMAD2. Int. J. Oncol. 54 (1), 306–314.

Owens, R.J., Baralle, F.E., 1986. Mapping the collagen-binding site of human fibronectin by expression in Escherichia coli. EMBO J. 5 (11), 2825–2830.

Paez-Ribes, M., et al., 2019. Targeting senescent cells in translational medicine. EMBO Mol. Med. 11 (12), e10234.

Paraskevopoulou, M.D., et al., 2013. DIANA-microT web server v5.0: service integration into miRNA functional analysis workflows. Nucleic Acids Res. 41 (Web Server issue), W169–W173.

Pitto, L., et al., 2009. miR-290 acts as a physiological effector of senescence in mouse embryo fibroblasts. Physiol. Genomics 39 (3), 210–218.

Qi, H., et al., 2017. Micro-RNA screening and prediction model construction for diagnosis of salt-sensitive essential hypertension. Medicine (Baltimore) 96 (17), e6417.

Qian, B., et al., 2020. MiR-361-5p exerts tumor-suppressing functions in gastric carcinoma by targeting syndecan-binding protein. Anti-Cancer Drugs 31 (2), 131–140.

Rahman, M., 2019. NemaLife: A Structured Microfluidic Culture Device Optimized for Aging Studies in Crawling C. elegans. BioRxiv.

Rahman, M., et al., 2020. NemaLife chip: a micropillar-based microfluidic culture device optimized for aging studies in crawling C. Elegans. Sci. Rep. 10 (1), 16190.

Ramasamy, R., Shekhtman, A., Schmidt, A.M., 2016. The multiple faces of RAGE–opportunities for therapeutic intervention in aging and chronic disease. Expert Opin. Ther. Targets 20 (4), 431–446.

Rani, A., et al., 2017. miRNA in circulating microvesicles as biomarkers for age-related cognitive decline. Front. Aging Neurosci. 9, 323.

Romo-Garcia, M.F., et al., 2019. Identification of putative miRNA biomarkers in early rheumatoid arthritis by genome-wide microarray profiling: a pilot study. Gene 720, 144081.

Schmauck-Medina, T., et al., 2022. New hallmarks of ageing: a 2022 Copenhagen ageing meeting summary. Aging (Albany NY) 14 (16), 6829–6839.

Schneider, F., Metz, I., Rust, M.B., 2022. Regulation of actin filament assembly and disassembly in growth cone motility and axon guidance. Brain Res. Bull. 192, 21–35.

Shen, B., et al., 2019. LncRNA MEG3 negatively modified osteosarcoma development through regulation of miR-361-5p and FoxM1. J. Cell. Physiol. 234 (8), 13464–13480.

Spinelli, R., et al., 2022. ZMAT3 hypomethylation contributes to early senescence of preadipocytes from healthy first-degree relatives of type 2 diabetics. Aging Cell 21 (3), e13557.

Su, M., et al., 2020. Circulating microRNA profiles based on direct S-Poly(T)Plus assay for detection of coronary heart disease. J. Cell. Mol. Med. 24 (11), 5984–5997.

Tentler, D., et al., 2019. Role of ACTN4 in tumorigenesis, metastasis, and EMT. Cells 8 (11).

Vander Ark, A., Cao, J., Li, X., 2018. TGF-beta receptors: in and beyond TGF-beta signaling. Cell. Signal. 52, 112–120.

Vlachos, I.S., et al., 2015. DIANA-miRPath v3.0: deciphering microRNA function with experimental support. Nucleic Acids Res. 43 (Web Server issue), W460–W466.

Voskamp, C., et al., 2021. TWIST1 controls cellular senescence and energy metabolism in mesenchymal stem cells. Eur. Cell. Mater. 42, 401–414.

Wang, A., et al., 2019. MEG3 promotes proliferation and inhibits apoptosis in osteoarthritis chondrocytes by miR-361-5p/FOXO1 axis. BMC Med. Genet. 12 (1), 201.

Watanabe, S., et al., 2017. Impact of senescence-associated secretory phenotype and its potential as a therapeutic target for senescence-associated diseases. Cancer Sci. 108 (4), 563–569.

van Willigenburg, H., de Keizer, P.L.J., de Bruin, R.W.F., 2018. Cellular senescence as a therapeutic target to improve renal transplantation outcome. Pharmacol. Res. 130, 322–330.

de Wit, E., et al., 2009. Repertoire and evolution of miRNA genes in four divergent nematode species. Genome Res. 19 (11), 2064–2074.

Wu, D., Prives, C., 2018. Relevance of the p53-MDM2 axis to aging. Cell Death Differ. 25 (1), 169–179.

Wu, X., et al., 2013. MicroRNA-361-5p facilitates cervical cancer progression through mediation of epithelial-to-mesenchymal transition. Med. Oncol. 30 (4), 751.

Yang, H.S., Hinds, P.W., 2003. Increased ezrin expression and activation by CDK5 coincident with acquisition of the senescent phenotype. Mol. Cell 11 (5), 1163–1176.

Yang, H.S., Hinds, P.W., 2006. Phosphorylation of ezrin by cyclin-dependent kinase 5 induces the release of rho GDP dissociation inhibitor to inhibit Rac1 activity in senescent cells. Cancer Res. 66 (5), 2708–2715.

Yang, J., et al., 2021. DIAPH1 promotes laryngeal squamous cell carcinoma progression through cell cycle regulation. Front. Oncol. 11, 716876.

Yang, W., Xie, T., 2020. Hsa_circ_CSPP1/MiR-361-5p/ITGB1 regulates proliferation and migration of cervical cancer (CC) by modulating the PI3K-akt signaling pathway. Reprod. Sci. 27 (1), 132–144.

Yin, L.C., et al., 2020. MicroRNA-361-5p inhibits tumorigenesis and the EMT of HCC by targeting Twist1. Biomed. Res. Int. 2020, 8891876.

Zhang, K., et al., 2020. The dichotomous role of TGF-beta in controlling liver cancer cell survival and proliferation. J. Genet. Genomics 47 (9), 497–512.

Zhang, X., et al., 2017. MicroRNA-361-5p inhibits epithelial-to-mesenchymal transition of glioma cells through targeting Twist1. Oncol. Rep. 37 (3), 1849–1856.

Zhang, Z., et al., 2018. Obesity-induced upregulation of miR-361-5p promotes hepatosteatosis through targeting Sirt1. Metabolism 88, 31–39.

Zheng, S.R., et al., 2021. circGFRA1 affects the sensitivity of triple negative breast cancer cells to paclitaxel via the miR-361-5p/TLR4 pathway. J. Biochem. 169 (5), 601–611.

Zhou, C., et al., 2020. COX10-AS1 facilitates cell proliferation and inhibits cell apoptosis in glioblastoma cells at post-transcription level. Neurochem. Res. 45 (9), 2196–2203.

Zhuang, Z.L., Tian, F.M., Sun, C.L., 2016. Downregulation of miR-361-5p associates with aggressive clinicopathological features and unfavorable prognosis in non-small cell lung cancer. Eur. Rev. Med. Pharmacol. Sci. 20 (24), 5132–5136.